Neutronics Analysis of Water-Cooled Ceramic Breeder Blanket for CFETR

2016 Plasma Sci. Technol. 18 775

(http://iopscience.iop.org/1009-0630/18/7/775)

Neutronics Analysis of Water-Cooled Ceramic Breeder Blanket for CFETR*

ZHU Qingjun (祝庆军)[1], LI Jia (李佳)[2], LIU Songlin (刘松林)[1]

[1]Institute of Plasma Physics, Chinese Academy of Sciences, Hefei 230031, China
[2]School of Nuclear Science and Technology, University of Science and Technology of China, Hefei 230027, China

Abstract In order to investigate the nuclear response to the water-cooled ceramic breeder blanket models for CFETR, a detailed 3D neutronics model with 22.5° torus sector was developed based on the integrated geometry of CFETR, including heterogeneous WCCB blanket models, shield, divertor, vacuum vessel, toroidal and poloidal magnets, and ports. Using the Monte Carlo N-Particle Transport Code MCNP5 and IAEA Fusion Evaluated Nuclear Data Library FENDL2.1, the neutronics analyses were performed. The neutron wall loading, tritium breeding ratio, the nuclear heating, neutron-induced atomic displacement damage, and gas production were determined. The results indicate that the global TBR of no less than 1.2 will be a big challenge for the water-cooled ceramic breeder blanket for CFETR.

Keywords: fusion reactor, WCCB blanket, TBR, nuclear heating

PACS: *28.52.Nh*

DOI: 10.1088/1009-0630/18/7/13

(Some figures may appear in colour only in the online journal)

1 Introduction

CFETR is an “ITER-like” Chinese Fusion Engineering Test Reactor whose conceptual design is being performed. The missions of physics and engineering are to generate 50–200 MW fusion power, and to realize 0.3–0.5 of duty time for burning plasma with a long pulse operation or steady state operation, at the same time, to achieve the tritium breeder ratio (TBR) for a blanket of no less than 1.2 [1]. The concept design of the water-cooled ceramic breeder (WCCB) blanket with superheated steam has been proposed as one candidate of CFETR breeding blankets [2,3].

The achievable TBR depends on the 3D geometrical configuration of the plasma chamber. While accurate modeling of the FW/blanket is the dominant factor, all other components in the plasma chamber will have an impact on the TBR [4,5]. In order to reduce the uncertainty caused by the geometry as much as possible, a detailed 3D neutronics model with a 22.5° torus sector, including heterogeneous WCCB blanket models, shield, divertor, vacuum vessel, thermal shield, toroidal and poloidal magnets, and ports, was developed based on the integrated conceptual design geometry of CFETR. This paper presents the nuclear analyses for the WCCB blanket using the Monte Carlo N-Particle Transport Code MCNP5 [6] and IAEA Fusion Evaluated Nuclear Data Library FENDL2.1 [7].

2 Neutronics models

The basic parameters of CFETR were defined as a major radius of 5.7 m, minor radius of 1.6 m, elongation of 1.8–2.0, and triangularity of 0.4–0.8. The development space (R ~5.9 m, a ~2 m, B_t=5 T, I_p ~14 MA) has been reserved for future device update. It mainly consists of a toroidal field coil (TFC), poloidal field coil (PFC), central solenoid (CS), vacuum vessel (VV), ports, cryostat, thermal shield, divertor, blanket, and shield. It has 16 large TFCs and 16 VV sectors. A WCCB with superheated steam [4] was proposed as the reference scheme. The 4 inboard blanket modules and 6 outboard blanket modules are arranged around the plasma. The toroidal dimension for each module is allocated according to the toroidal segmentation of 11.25°. The shield behind the blanket is divided into a high temperature shield (HTS) and a low temperature shield (LTS). The divertor employs a cassette structure with vertical targets and dome plates. Taking the toroidal distribution into account, there are 5 divertor segments in a VV sector. The material compositions of the main components for CFETR are listed in Table 1.

*supported by the National Magnetic Confinement Fusion Science Program of China (Nos. 2013GB108004, 2014GB122000, and 2014GB119000), and National Natural Science Foundation of China (No. 11175207)

Table 1. Main components material composition (Vol.%) for CFETR

Component name	Material composition	Component name	Material composition
Divertor W-armor	Tungsten 100%	Port plug	SS316LN: 60%; water: 40%
Divertor structure	SS316LN: 60%; water: 40%	PFC conductor	Epoxy: 10.7%; NbTi: 2.78%; CuNi: 0.21%; Ni: 0.25%; Cu: 20.86%; He: 16%; void: 1.9%
Inboard HTS	WC: 75%; SS316LN: 10%; H_2O: 15%	Blanket: FW W-armor	Tungsten 100%
Outboard HTS	SS316LN: 60%; water: 40%	Blanket: Side wall	H_2O: 20%, RAFM: 80%
LTS	WC: 75%; SS316LN: 10%; H_2O: 15%	Blanket: FW structure	Superheated steam: 25.3%; (density 0.051 g/cm^3); RAFM steel, 74.7%
VV IWS	H_2O: 41%; SS304B4: 36.9%; SS316LN: 15.9%; void: 3.4%; Ti-6Al-4V: 1.9%; Inconel 718: 0.5%	Blanket: Mixed breeding pebble bed	Breeder: Li_2TiO_3 18% Li6 enrichment 90% Multiplier: $Be_{12}Ti$ 80% Packing factor 0.65–0.8
VV shell	SS316LN: 100%	Blanket: Be pebble bed	100%, Packing factor 0.8
Thermal shield	SS316LN: 100%	Blanket: CP1–CP2	Boiling water 39.68% (density: 0.12 g/cm^3) RAFM steel 60.32%
Cryostat	SS316LN: 100%	Blanket: CP3–CP7	Saturated boiling water 39.68% (density: 0.481 g/cm^3); RAFM steek 60.32%
TFC case	SS 316L(N)-IG: 100%	Blanket: Reflector	H_2Zr 100%
TFC winding pack (WP)	SS316LN: 54.31%; Nb3Sn: 14.82%; Cu: 8.59%; Glass: 7.33%; He: 14.95%	Blanket: Stiffening plate	Saturated boiling water 39.68% (density: 0.481 g/cm^3); RAFM steel, 60.32%
TFC insulator	Cyanate ester resin C: 69%; H: 8.48%; O: 16%; N: 20.32%	Blanket: Back plate (BP)	H_2O: 20%, RAFM: 80%

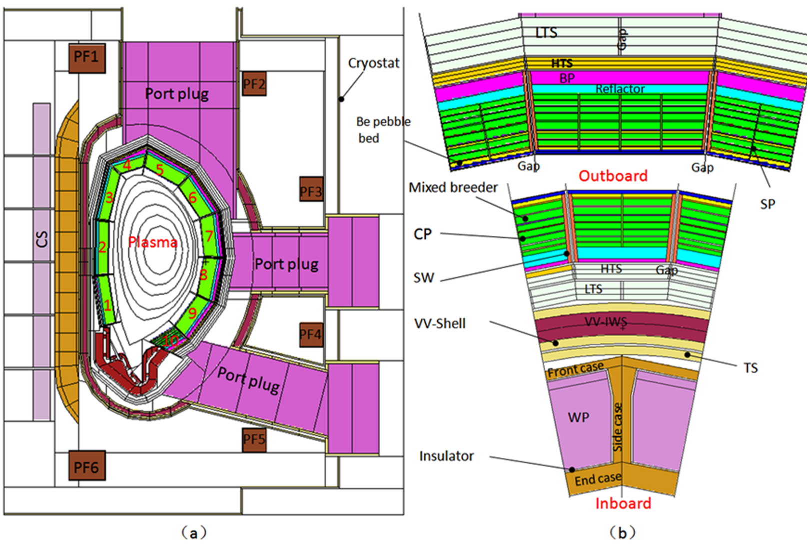

Fig.1 (a) Vertical cross section and (b) horizontal cross section of the CFETR neutronics model

Based on the integrated geometry of CFETR concept design, a 3D neutronics model with 22.5 degrees torus sector was developed. Fig. 1 shows a vertical cross section through the middle of the VV ports and a horizontal cross section at the inboard and outboard side. In order to avoid homogenization, the breeding blanket modules were created as detailed as possible, while some parts, including the mixture breeder pebble beds, first wall (FW), cooling plates (CP), back plates (BP), stiffening plates (SP), and side wall (SW) were assumed as homogenous material. For assembling blankets, the gaps between blanket modules at the toroidal and at the poloidal direction were set as 2 cm.

The five-nested DT neutron sources were built based on the Refs. [8, 9] and MHD equilibrium calculation (Fig. 2). The normalized neutron intensities of the five-nested neutron sources were 1%, 6%, 13%, 30%, and 50%, respectively, and the isotropic neutrons with Gaussian fusion spectra were distributed uniformly in each source.

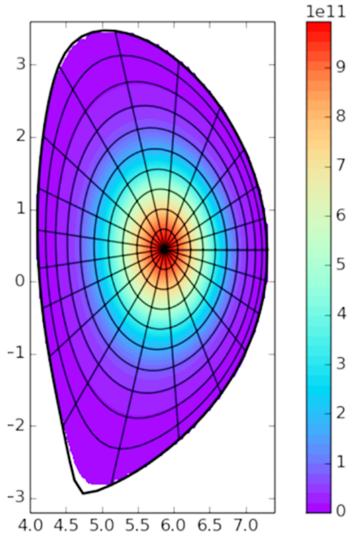

Fig.2 The five-nested DT neutron sources for 200 MW fusion power

3 Results and analysis

3.1 Neutron wall loading distribution

The neutron wall loading (NWL) is generally defined as current density, which is normalized to 200 MW fusion power, of uncollided 14 MeV neutrons crossing the FW [9]. In order to obtain detailed distribution of the NWL, the W-amour surface of the FW of the blanket modules and divertor plates was segmented. The NWL distribution was calculated and Fig. 3 shows the NWL poloidal distribution along the first wall line. The peak NWL of inboard and outboard is found in the equatorial plane. The inboard peak NWL value is 0.35 MW/m^2 and the outboard peak NWL is 0.44 MW/m^2. The peak NWL value of the divertor is 0.23 MW/m^2 which appears at two sides of the dome plate. The area of the FW surface for CFETR is about 632 m^2 including the divertor, thus the average NWL value is 0.31 MW/m^2.

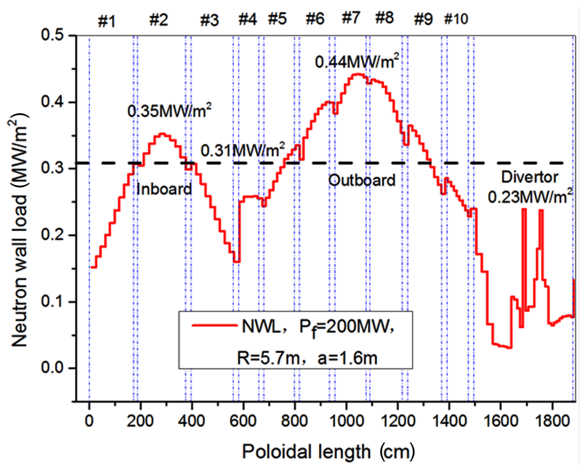

Fig.3 Neutron wall loading distribution on W-armor of blankets and divertor

3.2 Tritium breeding capability

The tritium breeding capability is an important target to achieve tritium self-sufficiency for CFETR. Under 200 MW fusion power, the tritium breeding capability was evaluated based on the WCCB blanket with superheated steam concept, which were performed to study the impact factors on the global tritium breeding ratio (TBR). These impact factors include the mixed breeder pebble bed packing factor, ^{6}Li enrichment in the ceramic breeder, and Li density in the breeder. Fig. 4(a) illustrates the global TBR varying with the above factors, when the blanket coverage is 100% excluding the divertor region, and the radial dimensions of the inboard and outboard blankets are 495 cm and 675 cm, respectively. It is noted that the global TBR can satisfy the requirements of no less than 1.2 for CFETR when the Li_4SiO_4 is employed as the breeder, the packing factor of the mixed breeder pebble bed is 0.8, and ^{6}Li enrichment is 80at.%. However, when Li_2TiO_3 is employed as the breeder, the global TBR is at the range of 1.11 to 1.16 under ^{6}Li enrichment of 90at.% and is at the range of 1.09 to 1.147 under ^{6}Li enrichment of 80at.%. Fig. 4(b) shows the distribution of the tritium production rate per volume in blanket modules in the case of a 0.8 packing factor and ^{6}Li 90at.% and using Li_2TiO_3 as the breeder. In addition, the TBR would further decrease when several blanket ports are occupied by the auxiliary heating system and diagnostics. When one equatorial port of 2.25 m (Pol.)×1.75 m (Tor.) is assumed for diagnostics or heating purposes instead of the blanket, the global TBR would decrease about 1.1%. If four equatorial ports are assumed to equip with the heating system and the diagnostics, the TBR could only reach to about 1.1. So the achieved TBR will be a great challenge for the mission of CFETR.

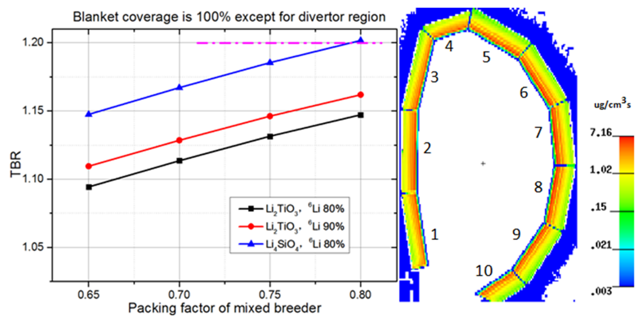

Fig.4 TBR varies with packing factor of mixture breeder (left); distribution of tritium production rate per volume in blanket modules for the case of 0.8 packing factor and ^{6}Li 90at.% and Li_2TiO_3 (right)

3.3 Nuclear heating power

The nuclear heating power of 218.33 MW was achieved. Table 2 shows the breakdown of nuclear heating into different components for 200 MW fusion power of CFETR. It is noted that about 90.5% and 8.5% fraction of the total nuclear heating was generated in the blanket modules and divertor, respectively, and 1.0% nuclear heating was deposited in the HTS and LTS. The nuclear heating fraction on the VV is very low. The possible reasons are that some penetration ways and assembly attachment gaps, and so on were omitted in the current conceptual design phase, and that a shield with WC material might provide better shielding performance.

Table 2. Nuclear heating power and energy multiplication

Component name	Nuclear heating power (MW)
Blanket	197.51
Divertor	18.62
High temperature shield	0.71
Low temperature shield	1.47
Vacuum vessel	0.02
Total	218.33
Energy multiplication	1.36

Table 3 also summarizes nuclear heating in the single blanket modules. It is obvious that the No.7 module captures maximum heating of 1001.42 kW. The energy multiplication factor is defined as the ratio of the total nuclear heating in all reactor components and the neutron power (200 MW×0.8) [10]. An energy multiplication of 1.36 was obtained for CFETR.

The neutron and photon heating density distributions on the blanket modules and the divertor were simultaneously obtained by using a mesh tally. The mesh tally value indicates an average over each mesh element combining the different material. Because of the limitation of element size and number, Fig. 5 only reflects a trend of the heating density distribution. However, it is observed that the main contribution to the nuclear heating density comes from neutrons inside blanket modules, especially in the breeder zone, but in the W armor of the blanket and divertor, the dominant heating contributor is the photon.

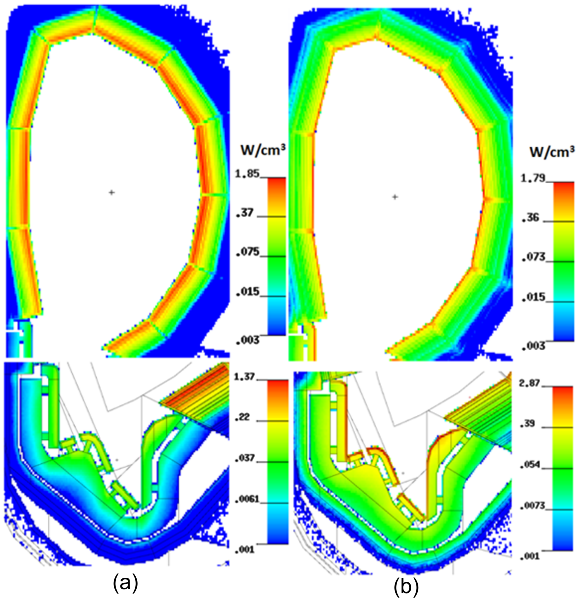

Fig.5 Distributions of the nuclear heating density generated by (a) neutron and (b) photon in blanket modules and divertor

3.4 Radiation damage

The damage to material caused by particle irradiation is an important design consideration in the fusion reactor. The neutron-induced atomic displacement damage accumulation in the W armor and Fe-based material of the blanket were calculated by employing NRT displacements per atom (DPA) model [11]. The gas (helium and hydrogen) accumulation was analyzed mainly based on (n,p) reactions for hydrogen production and (n,α) reactions for helium production in the material. The neutronics analyses were performed with the assumption of a duty time factor of 50% under 200 MW fusion power.

In one full power year (FPY), the maximum DPA of W and in RAFM steel, 0.59 and 2.74, were found in the No.7 module (Fig. 6(a)). Fig. 6(b) shows that DPA/FPY decreases dramatically with the distance away from the plasma.

Table 3. Nuclear heating power in the different single blanket modules and its main components

	Nuclear heating power (kW)								
Module No.	FW	SW	SP	CP	Breeder and multiplier zone	Reflector	BP	Total	Fraction
Blanket1	74.57	26.92	3.01	34.80	211.75	11.72	2.51	365.28	5.91%
Blanket2	95.17	39.49	4.51	50.36	353.69	16.76	3.32	563.21	9.12%
Blanket3	76.70	27.27	3.08	36.65	265.63	11.36	1.95	421.88	6.84%
Blanket4	49.72	15.27	5.32	24.86	178.98	9.80	4.64	288.35	4.67%
Blanket5	103.69	25.92	9.94	45.45	421.16	8.59	4.17	618.61	10.02%
Blanket6	138.49	29.55	11.72	63.78	585.94	12.64	6.34	845.17	13.74%
Blanket7	160.51	32.39	13.14	76.70	698.15	15.63	7.81	1001.42	16.28%
Blanket8	151.99	30.47	12.29	71.02	651.99	14.35	7.17	937.50	15.23%
Blanket9	121.45	25.78	10.16	54.26	500.71	10.37	5.25	731.53	11.80%
Blanket10	75.99	15.63	4.01	28.76	262.78	4.64	2.53	394.18	6.39%

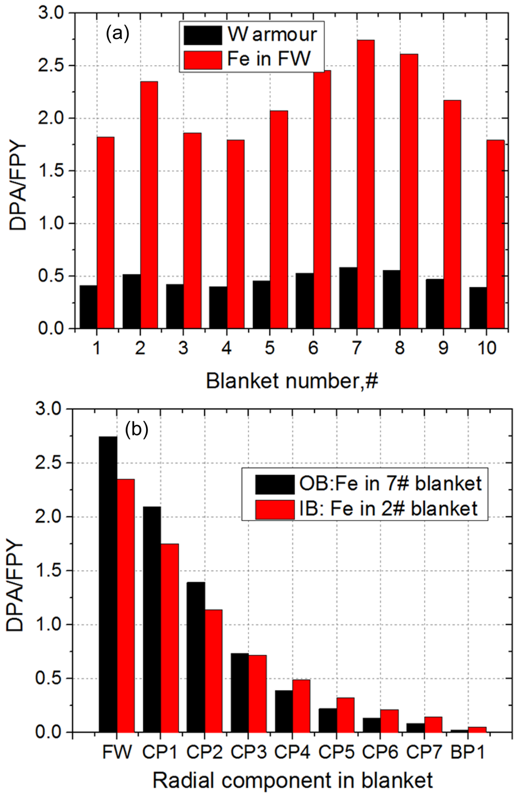

Fig.6 (a) DPA/FPY in W and Fe of the FW as a function of the poloidal location, (b) DPA/FPY in W and Fe in blanket module7 as a function of the radial location

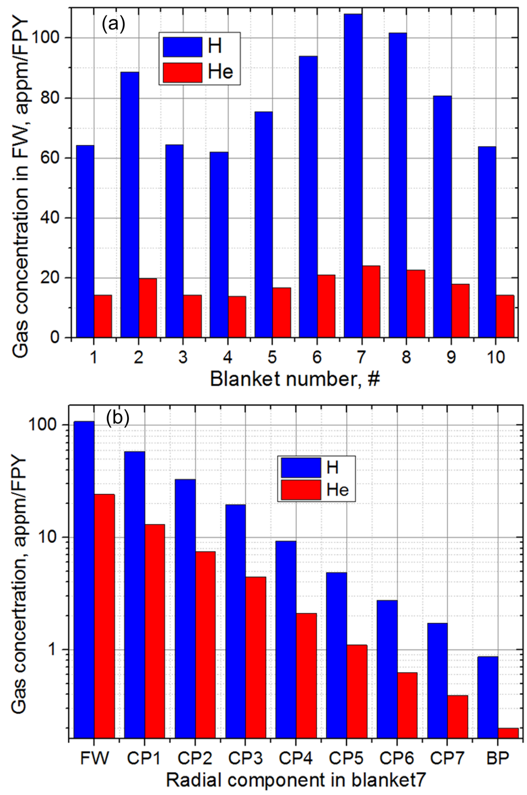

Fig.7 (a) Gas concentration in FW of blanket modules as a function of the radial location, (b) Gas concentration in RAFM steel in the No.7 blanket as a function of the poloidal location

The gas production per FPY in RAFM steel of blanket modules is illustrated in Fig. 7. It was observed that the peak H production rate was 10^7 appm/FPY and the peak He production rate was 24 appm/FPY in the RAFM steel of the No.7 module. The hydrogen and helium production rate in the RAFM steel structure components for the No.7 blanket also fell dramatically with the distance away from the plasma.

According to the literature [12], DPA and the gas production level in Fe-based material for the WCCB blanket with 200 MW fusion power are lower than the allowable requirement of RAFM material under 20 operation years with 50% of the duty time.

4 Summary

The neutronics analyses were performed to determine the nuclear performance parameters for the water-cooled ceramic breeder blanket of CFETR under 200 MW fusion power, based on the detailed 3D neutronics model and five-nested neutron source that are defined.

The results indicate that the outboard and inboard peak NWL on the FW line are 0.44 MW/m^2 and 0.35 MW/m^2, respectively. The TBR can only slightly achieve the required TBR of more than 1.2, only when Li_4SiO_4 is employed as the breeder, and the packing factor of the mixed pebble bed is 0.8, and ^{6}Li enrichment is 80at.%, as well as the blanket coverage being 100%. However, when one equatorial port of 2.2 m (Pol.)×1.75 m (Tor.) is assumed to be equipped with a heating or diagnostics system instead of a blanket, the TBR will decrease about 1.1%. So a TBR of no less than 1.2 will be a great challenge for the mission of CFETR. The nuclear heating power of 218.33 MW is achieved, leading to an energy multiplication of 1.36. The neutron-induced atomic displacement damage and gas production level in RAFM are lower than the allowable requirement of the RAFM material under 20 operation years with 50% of the duty time.

However, with the progress in components design, some penetration channels and assembly attachment gaps, and so on, need to be further focused on and modeled and analyzed in the future. The tritium breeding capability needs to be further optimized for the mission of CFETR.

References

1 Wan Yuanxi. 2013, Design and strategy for the Chinese fusion engineering testing reactor (CFETR). 25th symposium on fusion engineering (SOFE-25), San Francisco, CA, 2013: p.10-14

2 Liu Songlin, Pu Yong, Cheng Xiaoman, et al. 2014, Fusion Engineering and Design, 89: 1380

3 Ma Xuebin, Liu Songlin, Li Jia, et al. 2014, Plasma Science and Technology, 16: 390

4 Sawan M E, Abdou M A. 2006, Fusion Engineering and Design, 81: 1131

5 Li Jia, Zhang Xiaokang, Gao Fangfang, et al. 2016, Plasma Science and Technology, 18: 179

6 X-5 Monte Carlo Team. 2003, MCNP-A General Monte Carlo N-Particle Transport Code. Version 5, Volume I, MCNP Overview and Theory, Los Alamos National Laboratory, LA-UR-03-1987

7 Lopez Al-dama D, Trkov A. 2004, FENDL-2.1: update of an evaluated nuclear data library for fusion applications. Vienna: IAEA, Report INDC(NDS)-46

8 Fausser C, Puma A L, Gabriel F, et al. 2012, Fusion Engineering and Design, 87: 787

9 Polunovskiy E. 2008, D-T neutron emission rate for standard neutron source for ITER nuclear analysis with MCNP code. ITER org. doc. IDM no. INAR-005 (2008)

10 Chen Yixue, Fischer U, Pereslavtsev P, et al. 2003, The EU Power Plant Conceptual Study: Neutronic Design Analyses for Near Term and Advanced Reactor Models (Vol. 6763): FZKA

11 Edward A Read and Cassiano R E de Oliveira. 2011, A functional method for estimating DPA tallies in Monte Carlo calculations of light water reactor. International Conference on Mathematics and Computational Methods Applied to Nuclear Science and Engineering, American Nuclear Society (ANS), ISBN 978-85-63688-00-2

12 Gilbert M R, Dudarev S L, Nguyen-Manh D, et al. 2013, Journal of Nuclear Materials, 442: S755

(Manuscript received 2 August 2015)
(Manuscript accepted 26 November 2015)
E-mail address of ZHU Qingjun:
zhuqingjun@ipp.ac.cn